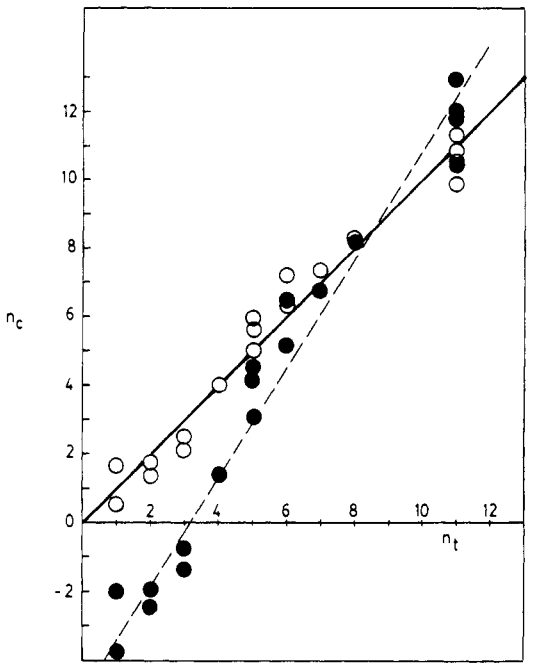

Figure 1. Number of conjugated C=C units in polyenes, n_c, as calculated with experimental ν_2 data and the exponential equation given in ref 1 (full circles) or that proposed here (empty circles), vs. the actual number of C=C units, n_t, in such polyenes. Solid line, equations $n_c = n_t$ and $n_c = 1.000079n_t - 0.001005$; dotted line, equation $n_c = 1.542n_t - 4.555$.

1). However, Maddams et al.[1] have already pointed out that such a reciprocal equation is not satisfactory.

In order to overcome the problems raised when the equation given by Maddams et al. is applied to the experimental data in Table I, an alternative way is proposed here to determine a and b, instead of the asymptotic regression method used by these authors. If the equation is written in logarithmic form as $\ln(\nu_2 - \nu) = \ln a - bn$, by plotting $\ln(\nu_2 - \nu)$ vs. n, a straight line with zero intercept $\ln a$ and slope $-b$ would be obtained; to carry out such a plot, the value of ν should be known beforehand from experimental measurements, and we have used the value of 1461 cm^{-1} given by Maddams et al., more widely experimentally supported than other values given by other authors. When the logarithmic form of the equation is applied with $\nu = 1461$ cm^{-1} to the experimental data in Table I, a straight line with $r = -0.98389$ is obtained, and the values $a = 215.76$ cm^{-1} and $b = 0.12036$ are thus calculated from the zero intercept and the slope, respectively. When these parameters are substituted in the exponential equation and $n_{C=C}$ is calculated for the ν_2 values in Table I, the results in Figure 1 (empty circles) are obtained. These data fit a straight line defined by the equation $n_c = 1.000079n_t - 0.001005$, with $r = 0.9839$; i.e., the calculated (n_c) values will be identical with the actual (n_t) values for $n_{C=C}$.

This same calculation has been performed with the limiting value $\nu = 1450$ cm^{-1} given by Lichtmann and Fitchen,[14] obtaining $a = 223.698$, $b = 0.108$, and $r = -0.98215$. The corresponding n_c vs. n_t plot leads to the equation $n_c = 0.99565\ n_t - 0.0342$, with $r = 0.9821$, slightly worse than that obtained above.

So, the equation $\nu_2 = 1461 + 215.76e^{-0.12036n}$ is proposed to determine the length of conjugated polyenes (as measured by the number of C=C units) from the ν_2 stretching frequency of such a moiety.

References and Notes

(1) Baruya, A.; Gerrard, D. L.; Maddams, W. F. *Macromolecules* **1983**, *16*, 578.
(2) Johnson, B. B.; Peticolas, W. L. *Annu. Rev. Phys. Chem.* **1976**, *27*, 465.
(3) Rives-Arnau, V.; Sheppard, N. *J. Chem. Soc., Faraday Trans. 1* **1980**, *76*, 394; **1981**, *77*, 953.
(4) Shorygin, P. P.; Ivanova, T. M. *Sov.-Phys.-Dokl. (Engl. Trans.)* **1963**, *8*, 493.
(5) Ivanova, T. M. *Opt. Spectrosc. (Engl. Trans.)* **1965**, *18*, 1975.
(6) Rimai, L.; Kilponen, R. G.; Gill, D. J. *J. Am. Chem. Soc.* **1970**, *92*, 3824.
(7) Behringer, J. In "Raman Spectroscopy"; Szimanskii, H., Ed.; Plenum Press: New York, 1967; Vol. 1, p 186, Table IV.
(8) Ivanova, T. M.; Yanovskaya, L. A.; Shorygin, P. P. *Opt. Spectrosc. (Engl. Trans.)* **1965**, *18*, 115.
(9) Sufrà, S.; Dellepiane, G.; Masetti, G.; Zebi, G. *J. Raman Spectrosc.* **1977**, *6*, 267.
(10) Harada, I.; Furukawa, Y.; Tasumi, M.; Shikawa, H.; Ikeda, S. *J. Chem. Phys.* **1980**, *73*, 4746.
(11) Lefrant, S.; Faulques, E.; Krichene, S.; Sagon, S. *Polym. Commun.* **1983**, *24*, 361.
(12) Kuzmany, H. *Phys. Stat. Solidi* **1980**, *B97*, 521.
(13) Kletter, M. J.; MacDiarmid, A. G.; Heeger, A. J.; Faulques, E.; Lefrant, S.; Bernier, P. *J. Polym. Sci., Polym. Lett. Ed.* **1982**, *20*, 211.
(14) Lichtmann, L. S.; Fitchen, D. B. *Synth. Met.* **1979/1980**, *1*, 139.

Communications to the Editor

Upper and Lower Critical Solution Temperature Behavior in Polymer Blends

It is well-known that most pairs of high molar mass polymers are immiscible. This is so because the combinatorial entropy of mixing of two polymers is dramatically less than that for two low molar mass compounds.[1] The enthalpy of mixing, on the other hand, is often a positive quantity. Therefore dissimilar polymers are only miscible if there are favorable specific interactions between them leading to a negative contribution to the Gibbs free energy of mixing. Miscible polymers tend to phase separate at elevated temperatures. This lower critical solution temperature (LCST) behavior is typical for miscible polymer blends. The LCST behavior is interpreted in terms of equation of state or free-volume contribution.[2,3] Some miscible polymers also exhibit phase separation at low temperatures. This upper critical solution temperature (UCST) behavior is rather uncommon. It has been observed only when one component has low molar mass, i.e., when one component is an oligomer.[4,5] So far, high molar mass polymers have been found to show only the LCST behavior.

Here we describe results for a mixture of high molar mass polymers which has been found to exhibit both UCST and LCST behavior. To our knowledge, this is the first observation of an UCST in polymer blends of high molar mass polymers.

The polymer specimens used in this study, BR and SBR-45, are commercial polymers supplied by Japan

0024-9297/85/2218-2089$01.50/0

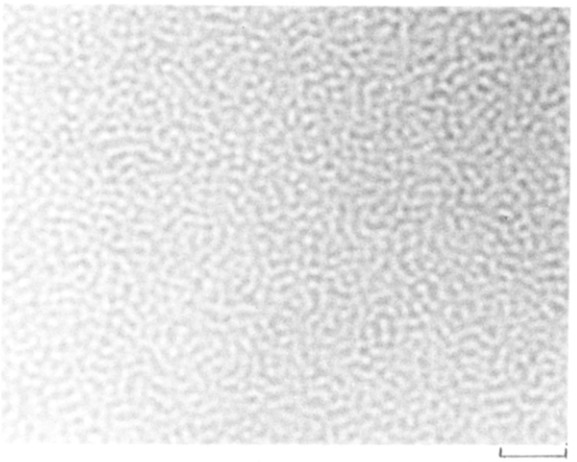

Figure 1. Light micrograph of 50/50 BR/SBR-45. Scale bar 10 μm.

Synthetic Rubber Co. Ltd. BR is a *cis*-1,4-polybutadiene prepared by solution polymerization with Ti catalyst (JSR BR02; $M_w = 39 \times 10^4$, $M_n = 18 \times 10^4$). SBR-45 is a poly(styrene-*co*-butadiene) containing 45% styrene prepared by emulsion polymerization (JSR SBR0202; $M_w = 48 \times 10^4$, $M_n = 16 \times 10^4$). These molecular weights were estimated by gel permeation chromatography calibrated with polystyrene standards.

BR and SBR-45 were dissolved at 8 wt % of total polymer in toluene. The solution was cast onto a cover glass (for microscopy). When the solvent was evaporated fairly quickly, a regularly phase-separated structure was formed in the cast film, as discussed in our recent article.[6] Figure 1 is a typical example of the light micrograph of the cast film of 50/50 BR/SBR-45. A highly interconnected two-phase morphology with uniform domain size is seen in the micrograph. We call it a "modulated structure",[6] partly for convenience to describe the morphological features of the unique periodicity and the high level of phase connectivity.

The cast film was further dried under vacuum (10^{-4} mmHg) for 10 h. Then the film on the cover glass was inserted in a heating stage (Linkam TH600 heating–cooling stage, Linkam Scientific Instruments, Ltd.[7]). This stage can be programmed to provide isothermal settings and also a linear rise in temperature at any of 27 different rates between 0.1 and 90 °C/min. The heating stage was set horizontally on the light scattering stage.[6] A He–Ne gas laser beam of 632.8-nm wavelength was applied vertically to the film specimen. A goniometer trace of the scattered light from the film was recorded during heating at a constant rate. Similar experiments were carried out at different heating rates. The light scattering profile from the film with the modulated structure had a peak (e.g., see Figure 4). The Bragg spacing from the peak angle corresponds to the periodic distance of the modulated structure in the micrograph.

When temperature was elevated, the light scattering profile did not change up to a certain temperature T_d. Above T_d the scattered intensity decreased with temperature, keeping the scattering peak angle almost constant. Then the scattering peak finally disappeared. A typical example is shown in Figure 2. T_d corresponds to the onset temperature of phase dissolution, as discussed later. T_d varied with heating rate. Selected results of T_d vs. heating rate plots are shown in Figure 3. The intercept of T_d, at which the heating rate is zero, may correspond to the binodal temperature. Similar experiments were carried out for blend specimens with various compositions. The binodal points thus estimated are indicated by open circles in Figure 4. An UCST-type phase diagram for the BB/SBR-45 system is drawn in Figure 4.

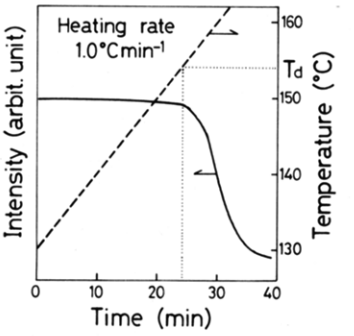

Figure 2. Change in the peak intensity of scattered light during heating at a constant rate of 1 °C/min, obtaining T_d. 50/50 BR/SBR-45.

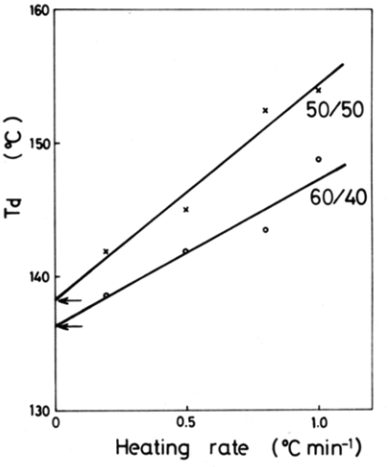

Figure 3. T_d vs. heating rate plots.

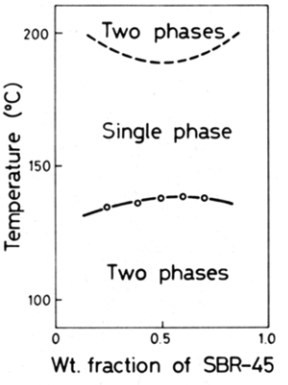

Figure 4. Phase diagram.

In order to confirm the UCST behavior, we carried out isothermal experiments as follows. The film specimen with the modulated structure was allowed to undergo a rapid temperature jump from room temperature to various higher temperatures set isothermally below and above the UCST. Below the UCST, no appreciable change in the scattering profile with time of isothermal annealing could be detected on a time scale of 2 h. This means that appreciable structural change did not take place. On the other hand, above the UCST the scattered intensity decreased with time of annealing, keeping the peak angle constant. A typical example is shown in Figure 5. This type of decay in the scattered intensity has been already discussed by Hashimoto et al.[8] for the case of small-angle X-ray scattering studies on the order-to-disorder transition of block copolymer. They have formulated the decay of

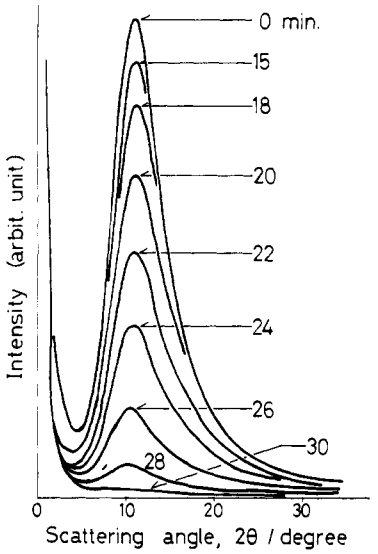

Figure 5. Change of light scattering profile with annealing at 155 °C. Figures are times after temperature jump. 30/70 BR/SBR-45.

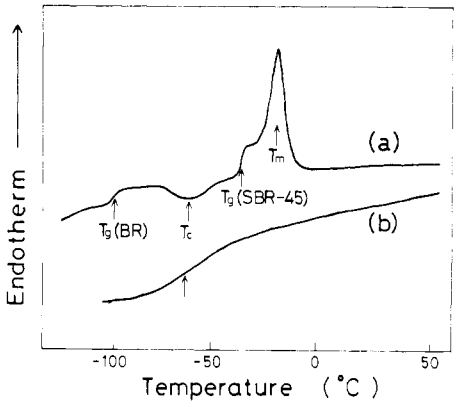

Figure 6. DSC thermograms: (a) as-cast film; (b) film annealed at 155 °C for 30 min. 50/50 BR/SBR-45.

the scattered intensity with variation of the concentration profile in microdomain structure from a regular two-phase structure with a sharp interface to that with a broad interface, eventually resulting in a uniform concentration distribution. On the basis of their formulation, the intensity decay in Figure 5 corresponds to the phase dissolution of the modulated structure, keeping the periodic distance constant, when the thermodynamic driving force for the phase separation is suddenly removed by the temperature jump from the two-phase region to the one-phase region. The kinetic aspect of the phase dissolution is an interesting problem. It is however beyond the scope of this paper and will be presented elsewhere.

The single-phase nature after the phase dissolution was confirmed by DSC studies. Curve a in Figure 6 is a DSC thermogram of the as-cast film of the 50/50 blend having a modulated structure. We see two glass transitions at the glass transition points of BR and SBR-45, respectively, and also a crystallization exotherm peak and a melting endotherm peak of BR. These transition features are nothing but the indication of the two-phase nature in the as-cast film. After the DSC run to get the thermogram a, the film specimen was further heated to 155 °C in the DSC pan and was annealed at that temperature for 30 min[10] and then rapidly quenched to liquid nitrogen temperature. The DSC thermogram of the annealed and quenched specimen is shown as curve b in Figure 6. All of the transitions in the as-cast film have disappeared. A broad, single glass transition is seen between the glass transition temperatures of BR and SBR-45. This implies that the two-phase structure was transformed to an almost homogeneous solution; in other words, phase dissolution took place by annealing above UCST.

For the investigation of the phase behavior at higher temperatures, the gradual heating procedure used for the study of the UCST was not appropriate. This was due to deterioration of the specimen by long exposure to the high-temperature atmosphere during the slow heating process. Instead, we employed a dissolution and temperature-jump procedure: the cast film was annealed above UCST, e.g., at 150 °C for ca. 30 min; then the annealed specimen underwent a rapid temperature jump to an isothermal setting of higher temperatures and the structural change was observed under the microscope and by using the light scattering technique. When no appreciable change took place, we judged that the system was still in the single-phase region. On the other hand, when the film became opaque and the scattering intensity increased, we judged that the system was in the two-phase region. On the basis of these observations, the LCST line was drawn somewhat arbitrarily in Figure 4. Actually we observed development of a modulated structure during isothermal annealing at the two-phase region above the LCST. It was similar in appearance to that in Figure 1 but the periodic distance of the structure was much smaller than the original one in the cast film. This implies that the structural memory in the cast film had disappeared by annealing in the single-phase region and a new concentration fluctuation developed by spinodal decomposition induced thermally above the LCST.

Thus we have found the coexistence of the UCST and LCST in the BR/SBR-45 system. This is not specific to this particular pair. Similar phase behavior was also found by us in other pairs of high molar mass polymers, such as BR/SBR-23 and poly(acrylonitrile-*co*-styrene)/poly(acrylonitrile-*co*-butadiene).[9] It seems to be a rather general phenomenon for some classes of homopolymer/copolymer and copolymer/copolymer systems. However, it is hard to interpret in the framework of current theories on polymer–polymer miscibility.[2,3] Recent ideas of "miscibility windows" for polymer blends including copolymer(s) can interpret miscibility and LCST behavior without any specific interaction.[11-14] They could be applied to interpret also the UCST behavior with minor modification. Another promising approach may be given by some modification of the equation of state theory.

Acknowledgment. We acknowledge partial support by the Scientific Research Fund (Kagaku-Kenkyu-hi 58470079) of the Ministry of Education, Japan, and a grant from the Japan Synthetic Rubber Co. Ltd., Tokyo, Japan. We are also deeply indebted to the Japan Society for Promotion of Science for supporting H.W.K. at the Tokyo Institute of Technology.

Registry No. (Acrylonitrile)·(styrene) (copolymer), 9003-54-7.

References and Notes

(1) Flory, P. J. "Principles of Polymer Chemistry"; Cornell University Press: Ithaca, NY, 1953.
(2) Paul, D. R., Newman, S., Eds. "Polymer Blends"; Academic Press: New York, 1978; Vol. 1.
(3) Olabisi, O.; Robeson, L. M.; Shaw, M. T. "Polymer–Polymer Miscibility"; Academic Press: New York, 1979.
(4) Roe, R. J.; Zin, W. C. *Macromolecules* **1980**, *13*, 1221.
(5) Zachaius, S. L.; ten Brinke, G.; MacKnight, W. J.; Karasz, F. E. *Macromolecules* **1983**, *16*, 381.
(6) Inoue, T.; Ougizawa, T.; Yasuda, O.; Miyasaka, K. *Macromolecules* **1985**, *18*, 57.
(7) Shephered, T. *Econ. Geol.* **1981**, *76*, 1244.

(8) Hashimoto, T.; Tsukahara, J.; Kawai, H. *Macromolecules* **1981**, *14*, 708.
(9) Preliminary results in our laboratory (by T. Ougizawa et al.).
(10) Note that the annealing conditions are identical with those of the longest case in Figure 4, at which the scattering peak has disappeared.
(11) Kambour, R. P.; Bendler, J. T.; Bopp, R. C. *Macromolecules* **1983**, *16*, 753.
(12) ten Brinke, G.; Karasz, F. E.; MacKnight, W. J. *Macromolecules* **1983**, *16*, 1827.
(13) Paul, D. R.; Barlow, J. W. *Polymer* **1984**, *25*, 487.
(14) The B unit in BR is different from that in SBR. The B unit in BR is cis-1,4 (solution polymerization). On the contrary, B units in SBR are composed of cis-1,4 (13%), trans-1,4 (69%), and vinyl (18%) (emulsion polymerization). B in SBR (=B′) ≠ B in BR. That is, our system is (B homopolymer)/(B′S random copolymer).

Toshiaki Ougizawa, Takashi Inoue,* and Hans W. Kammer

Department of Textile and Polymeric Materials
Tokyo Institute of Technology
Ookayama, Meguro-ku, Tokyo 152, Japan

Received June 13, 1985

Direct Observations of Macroperoxyl Radical Propagation and Termination by Electron Spin Resonance and Infrared Spectroscopies†

Numerous investigations have been made of the behavior of peroxyl radicals in oxidizing polymers.[1-8] These studies have depended heavily on the use of electron spin resonance (ESR) spectroscopy, which has great sensitivity for free radical species. However, the method is blind to nonradical species, which, in fact, constitute the bulk of the oxidation products. Nevertheless, the ESR observation of the decay of peroxyl radicals ($PO_2\cdot$) under vacuum to form macroalkyl radicals has been cited as direct evidence for the peroxyl propagation reaction 1.[1,2,5,7] In addition

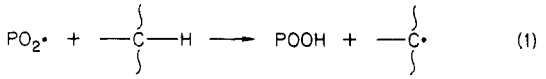

(1)

the conversion of an initially ^{17}O-labeled peroxyl population to ^{16}O peroxyl radicals in an $^{16}O_2$ atmosphere has been suggested to be definitive for this propagation (sequence 2).[6] Although, many of these studies refer to polypropylene (PP), both ESR methods ignore the very real possibility of macroalkyl formation without the intermediacy of the propagation step (reaction 1). This can result from *tert*-peroxyl self-reactions (reaction 3), which occur

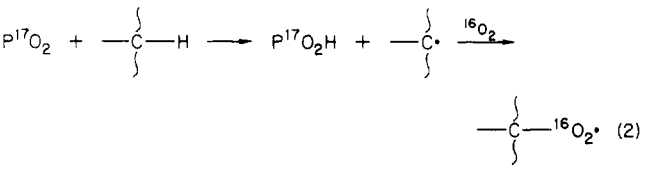

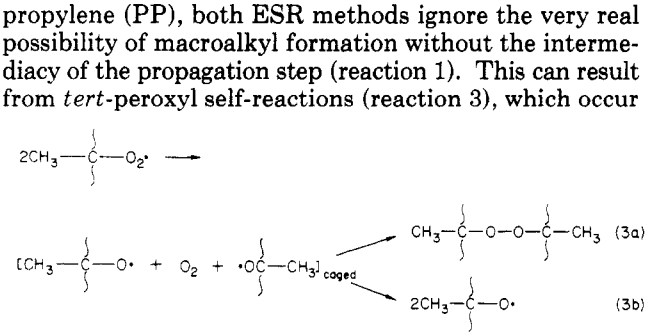

with a high probability in the early life of a radical pair or cluster.[3,5] As well as dimerization to give a peroxide cross-link, the reactive macroalkoxyl radicals produced in *tert*-peroxyl self-reaction are expected to either hydrogen abstract from the polymer to form macroalkyl radicals or undergo β-scission to form macroalkyl radicals (reaction 4). In both these cases these macroalkyls will then combine with O_2 to re-form peroxyls.

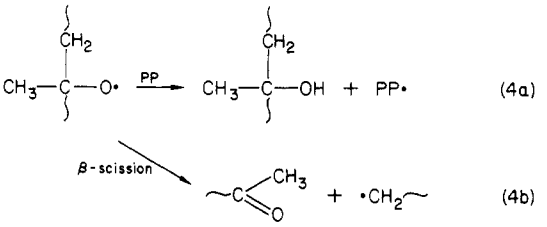

(4a) (4b)

Other evidence for the occurrence of the oxidative propagation steps (reaction sequence 2) in solid polymers comes from the indirect method of product analysis after appreciable oxidation.[3,4] In an attempt to obtain more direct evidence for the behavior of macroperoxyl radicals (both propagation and termination) and to resolve the potential ambiguity in the ESR approach, we have combined ESR and Fourier transform infrared (FTIR) spectroscopy to study both the decay of the polypropylene peroxyl ($PPO_2\cdot$) population and the associated formation of oxidation products. Although FTIR lacks the sensitivity of ESR, relatively high concentrations of $PPO_2\cdot$ can be generated by the γ-irradiation of PP in the presence of O_2 at −78 °C, conditions under which these radicals can neither propagate nor terminate. If these $PPO_2\cdot$ radicals are then allowed to propagate and terminate by suddenly warming above the PP T_g, we have found it possible to record the IR spectra of oxidation products as they accumulate from time zero. De Vries et al. have previously combined ESR and FTIR in the study of polyethylene oxidation but only reported the radical level at 77 K immediately after γ-irradiation and measured a single spectrum of the oxidized polymer after storage at room temperature, ignoring the decay process.[8]

Isotactic PP film (iPP, ~30-μm thickness unoriented, Hercules resin, exhaustively extracted to remove processing additives) and ~50 mg of pellets of atactic PP (aPP, Gulf resin, reprecipitated from toluene) or aPP coatings (~140 μm) on one surface of NaCl disks were exposed in an AECL Gamma cell 220 (^{60}Co, 1.35 Mrd·h^{-1}). During irradiation, the tubes containing PP samples in O_2 or air were refrigerated at −78 °C in solid carbon dioxide. The ESR spectra were recorded on prerolled scrolls of iPP film or on the aPP pellets after transfer at 77 K to fresh (color-center free) ESR tubes. The spectrometer was a Varian E4, equipped with a Nicolet 1170 integration system which was standardized both with an in-cavity ruby signal and known quantities of 2,2-diphenyl-1-picrylhydrazyl solution. Peroxyl signals were quantified at 10-mW microwave power (well below the saturation limit) but signals from macroalkyl-containing samples were found to require ≤1.0 mW to prevent detector saturation. Some aPP pellets showed a residual macroalkyl ESR signal immediately after irradiation in air in addition to the expected the $PPO_2\cdot$ signal, and were held at −78 °C until O_2-diffusion converted these radicals to $PPO_2\cdot$. At the dose rate used, all iPP films showed only a $PPO_2\cdot$ ESR signal.

FTIR spectra were recorded on separately irradiated iPP film samples (clamped flat in five layers on aluminum frames) and on the aPP-coated NaCl disks. Samples for FTIR were maintained at ≤−78 °C after γ-irradiation and transferred into the spectrometer at ≤−60 °C. A "zero-time" spectrum (prior to $PPO_2\cdot$ reaction) was then measured at −60 °C. To eliminate interference ripples from the iPP films, films were inclined at 56° (the Brewster

† Issued as NRCC No. 24877.

0024-9297/85/2218-2092$01.50/0 Published 1985 by the American Chemical Society